# Dynamic holographic optical tweezers

## Jennifer E. Curtis, Brian A. Koss, David G. Grier *

*James Franck Institute and Institute for Biophysical Dynamics, University of Chicago, 5640 S. Ellis Ave., Chicago, IL 60637, USA*

## Abstract

Optical trapping is an increasingly important technique for controlling and probing matter at length scales ranging from nanometers to millimeters. This paper describes methods for creating large numbers of high-quality optical traps in arbitrary three-dimensional configurations and for dynamically reconfiguring them under computer control. In addition to forming conventional optical tweezers, these methods also can sculpt the wavefront of each trap individually, allowing for mixed arrays of traps based on different modes of light, including optical vortices, axial line traps, optical bottles and optical rotators. The ability to establish large numbers of individually structured optical traps and to move them independently in three dimensions promises exciting new opportunities for research, engineering, diagnostics, and manufacturing at mesoscopic lengthscales. © 2002 Elsevier Science B.V. All rights reserved.

*PACS:* 42.40.Jv; 87.80.Cc

An optical tweezer uses forces exerted by intensity gradients in a strongly focused beam of light to trap and move a microscopic volume of matter [1]. Optical tweezers' unique ability to manipulate matter at mesoscopic scales has led to widespread applications in biology [2,3], and the physical sciences [4]. This paper describes how computer-generated holograms can transform a single laser beam into hundreds of independent optical traps, each with individually specified characteristics, arranged in arbitrary three-dimensional configurations. The enhanced capabilities of such dynamic holographic optical trapping

systems offer new opportunities for research and engineering, as well as new applications in biotechnology, nanotechnology, and manufacturing.

Holographic optical tweezers (HOT) use a computer-designed diffractive optical element (DOE) to split a single collimated laser beam into several separate beams, each of which is focused into an optical tweezer by a strongly converging lens [5–7]. Originally demonstrated with microfabricated DOEs [8], holographic optical tweezers have since been implemented with computer-addressed liquid crystal spatial light modulators [9,10]. Projecting a sequence of computer-designed holograms reconfigures the resulting pattern of traps. Unfortunately, calculating the phase hologram for a desired pattern of traps is not straightforward, and the lack of appropriate algorithms has prevented dynamic holographic op-

---
* Corresponding author. Tel.: +1-773-702-9176; fax: +1-773-702-5863.

*E-mail address:* d-grier@uchicago.edu (D.G. Grier).

tical tweezers from achieving their potential. This paper introduces new methods for computing phase holograms for optical trapping and demonstrates their use in a practical dynamic holographic optical trapping system.

The same optical gradient forces exploited in conventional optical tweezers [1] also operate in holographic optical tweezers. A dielectric particle approaching a focused beam of light is polarized by the light's electric field and then drawn up intensity gradients toward the focal point. Radiation pressure competes with this optical gradient force and tends to displace the trapped particle along the beam's axis. For this reason, optical tweezers usually are designed around microscope objective lenses whose large numerical apertures and minimal aberrations optimize axial intensity gradients.

An optical trap can be placed anywhere within the objective lens' focal volume by appropriately selecting the input beam's propagation direction and degree of collimation. For example, a collimated beam passing straight into an infinity-corrected objective lens comes to a focus in the center of the lens' focal plane, while another beam entering at an angle comes to a focus proportionately off-center. A slightly diverging beam focuses downstream of the focal plane while a converging beam focuses upstream. By the same token, multiple beams simultaneously entering the lens' input pupil each form optical traps in the focal volume, each at a location determined by its angle of incidence and degree of collimation. This is the principle behind holographic optical tweezers.

Our implementation, shown schematically in Fig. 1, uses a Hamamatsu X7550 parallel-aligned nematic spatial light modulator (SLM) [11] to reshape the beam from a frequency-doubled Nd:YVO$_4$ laser (Coherent Verdi) into a designated pattern of beams. Each is transferred by relay optics to the entrance pupil of a 100× NA 1.4 oil immersion objective mounted in a Zeiss Axiovert S100TV inverted optical microscope and then focused into a trap. A dichroic mirror reflects the laser light into the objective while allowing images of the trapped particles to pass through to a video camera. When combined with a 0.63× widefield video eyepiece, this optical train offers a 85 × 63 μm$^2$ field of view.

The Hamamatsu SLM can impose selected phase shifts on the incident beam's wavefront at each 40 μm wide pixel in a 480 × 480 array. The SLM's calibrated phase transfer function offers 150 distinct phase shifts ranging from 0 to 2π at the operating wavelength of λ = 532 nm. The phase shift imposed at each pixel is specified through a computer interface with an effective refresh rate of 5 Hz for the entire array. Quite sophisticated trapping patterns are possible despite the SLM's inherently limited spatial bandwidth. The array of 400 functional optical traps shown in Fig. 1 is the largest created by any means. Improvements in the number and density of effective phase pixels, in their diffraction efficiency, in the resolution of the available phase modulation, and in the refresh rate for projecting new phase patterns will correspondingly improve the performance of dynamic holographic optical tweezer systems. Other phase modulating technologies, such as micromirror arrays could offer the additional benefit of creating optical traps in multiple wavelengths simultaneously.

Modulating only the phase and not the amplitude of the input beam is enough to establish any desired intensity pattern in the objective's focal volume and thus any pattern of traps [7]. Such intensity-shaping phase gratings are often referred to as kinoforms. Previously reported algorithms for computing optical trapping kinoforms produced only two-dimensional distributions of traps [7,9] or patterns on just two planes [10]. Moreover, the resulting traps were suitable only for dielectric particles in low-dielectric media, and could not be adapted to handle metallic particles or samples made of absorbing, reflecting, or low-dielectric-constant materials. A more general approach relaxes all of these restrictions.

We begin by modeling the incident laser beam's electric field $E_0(\vec{\rho}) = A_0(\vec{\rho}) \exp(i\psi)$, as having constant phase, $\psi = 0$ in the DOE plane, and unit intensity: $\int_\Omega |A_0(\vec{\rho})|^2 \, d^2\rho = 1$. Here $\vec{\rho}$ denotes a position in the DOEs aperture $\Omega$, $A_0(\vec{\rho})$ is the real-valued amplitude profile of the input beam. The DOE then imposes a phase modulation $\varphi(\vec{\rho})$ onto the input beam's wavefront which, in principle, encodes the desired pattern of outgoing beams.
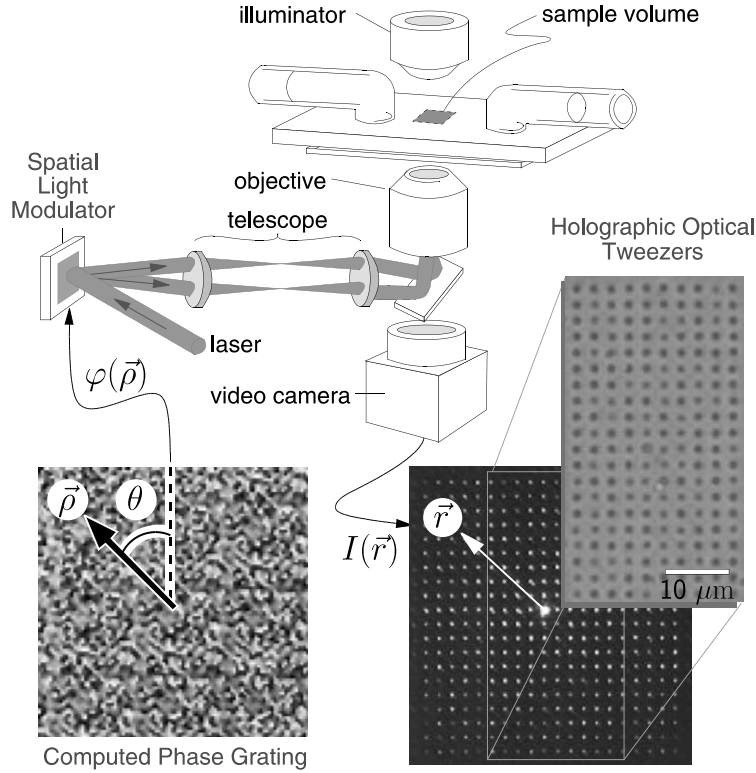
Fig. 1. Schematic implementation of dynamic holographic optical tweezers using a reflective liquid crystal spatial light modulator. The inset phase grating is 1/25 of the hologram $\varphi(\vec{\rho})$ encoding a $20 \times 20$ array of traps, with white regions corresponding to local phase shifts of $2\pi$ radians and black to 0. A telescope relays the diffracted beams to a high-numerical-aperture objective which focuses them into optical traps. The sample, enclosed in a glass flow cell, can be imaged through conventional video microscopy. The inset video micrograph shows the intensity $I(\vec{r}) = \sum_j |\epsilon_j|^2 \delta(\vec{r} - \vec{r}_j)$ of light from the traps reflected off a mirror temporarily placed in the object plane. The smaller inset shows these traps in action, holding two hundred colloidal polystyrene spheres, each 800 nm in diameter.

The electric field $\epsilon_j = \alpha_j \exp(\mathrm{i}\phi_j)$ at each of the discrete traps is related to the electric field $E(\vec{\rho})$ in the plane of the DOE by a generalized Fourier transform

$$E(\vec{\rho}) = \sum_{j=1}^{N} \int \epsilon_j \delta(\vec{r} - \vec{r}_j) K_j^{-1}(\vec{r}, \vec{\rho})$$

$$\times \exp\left(\mathrm{i}\frac{2\pi\vec{r} \cdot \vec{\rho}}{\lambda f}\right) \mathrm{d}^3 r$$

$$= \sum_{j=1}^{N} \epsilon_j K_j^{-1}(\vec{r}_j, \vec{\rho}) \exp\left(\mathrm{i}\frac{2\pi\vec{r}_j \cdot \vec{\rho}}{\lambda f}\right), \qquad (1)$$

$$\equiv A(\vec{\rho}) \exp(\mathrm{i}\varphi(\vec{\rho}), \qquad (2)$$

where $f$ is the effective focal length of the optical train, including the relay optics and objective lens.

The kernel $K_j(\vec{r}, \vec{\rho})$ can be used to transform the $j$th trap from a conventional tweezer into another type of trap, and $K_j^{-1}$ is its inverse. For conventional optical tweezers in the focal plane, $K_j = 1$.

If the calculated amplitude, $A(\vec{\rho})$, were identical to the laser beam's profile, $A_0(\vec{\rho})$, then $\varphi(\vec{\rho})$ would be the kinoform encoding the desired array of traps. Unfortunately, this is rarely the case. More generally, the spatially varying discrepancies between $A(\vec{\rho})$ and $A_0(\vec{\rho})$ direct light away from the desired traps and into ghosts and other undesirable artifacts. Despite these shortcomings, combining kinoforms with Eq. (1) is expedient and can produce useful trapping patterns [10]. Still better and more general results can be obtained by using Eqs. (1) and (2) as the basis for an iterative search for the ideal kinoform.

Following the approach pioneered by Gerchberg and Saxton (GS) [12], we treat the phase $\varphi(\vec{\rho})$ calculated with Eqs. (1) and (2) as an estimate, $\varphi^{(n)}(\vec{\rho})$, for the desired kinoform and use this to calculate the fields at the trap positions given the laser's actual profile $A_0(\vec{\rho})$

$$\epsilon_j^{(n)} = \int_\Omega A_0(\vec{\rho}) \exp(\mathrm{i}\varphi^{(n)}(\vec{\rho})) K_j(\vec{r}_j, \vec{\rho})$$
$$\times \exp\left(-\mathrm{i}\frac{2\pi\vec{r}_j \cdot \vec{\rho}}{\lambda f}\right) \mathrm{d}^2\rho. \tag{3}$$

The index $n$ refers to the $n$th iterative approximation to $\varphi(\vec{\rho})$.

The classic GS algorithm replaces the amplitude $\alpha_j^{(n)}$ in this estimate with the desired amplitude $\alpha_j$, leaving the corresponding phase $\phi_j^{(n)}$ unchanged, and solves for the next estimate $\varphi^{(n+1)}(\vec{\rho})$ using Eqs. (1) and (2). The fraction $\sum_j |\alpha_j^{(n)}|^2$ of the incident power actually delivered to the traps by the $n$th approximation is useful for tracking the algorithm's convergence.

For the present application, the simple GS substitution leads to slow and non-monotonic convergence. We find that an alternate replacement scheme

$$\alpha_j^{(n+1)} = \left[(1-\xi) + \xi\frac{\alpha_j}{\alpha_j^{(n)}}\right]\alpha_j \tag{4}$$

leads to rapid monotonic convergence for $\xi \approx 0.5$. The resulting estimate for $\varphi(\vec{\rho})$ then can be discretized and transmitted to the SLM to establish a trapping pattern. In cases where the SLM offers

only a few distinct phase levels, discretization can be incorporated into each iteration to minimize the associated error. In all of the examples discussed below, this algorithm yields kinoforms with theoretical efficiencies exceeding 80% in two or three iterations starting from a random choice for the traps' initial phases $\phi_j$ and often converges to solutions with better than 90% efficiency. Iterative optimization with Eqs. (2) and (3) is computationally efficient because discrete transforms are calculated only at the actual trap locations.

Fig. 2(a) shows 26 colloidal silica spheres 0.99 μm in diameter suspended in water and trapped in a planar fivefold pattern of optical tweezers created with Eqs. (2) and (3). Replacing this kinoform with another whose traps are slightly displaced moves the spheres into the new configuration. Projecting a sequence of trapping patterns translates the spheres deterministically into an entirely new configuration. Fig. 2(b) shows the same spheres after 16 such hops, and Fig. 2(c) after 38. Powering each trap with 1 mW of light traps the particles stably against thermal forces. Increasing the trapping power to 10 mW and updating the trapping pattern in 2 μm steps allows us to translate particles at up to 10 μm/s.

Comparable planar motions also have been implemented by rapidly scanning a single tweezer through a sequence of discrete locations, thereby creating a time-shared trapping pattern [13]. The continuous illumination of holographic optical traps offer several advantages, however. HOT patterns can be more extensive both spatially and
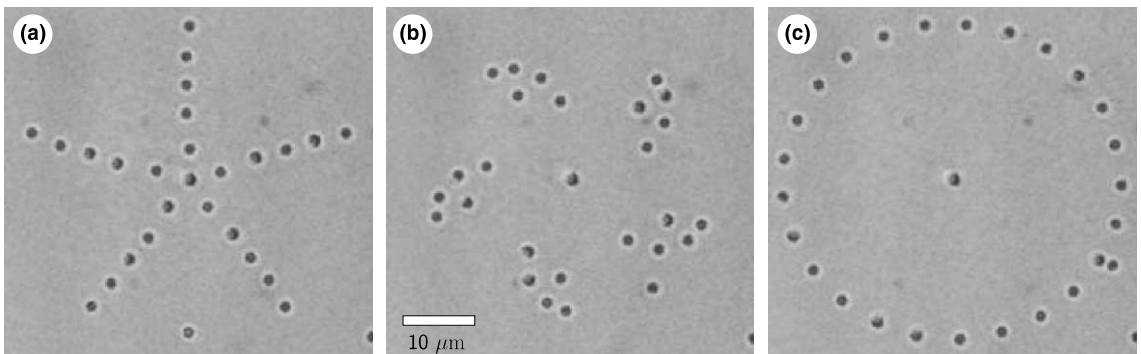


Fig. 2. A fivefold pattern of 26 colloidal silica spheres 0.99 μm in diameter is transformed into a circle using dynamic holographic optical tweezers. (a) The original configuration; (b) after 16 steps; (c) the final configuration after 38 steps.

in number of traps than time-shared arrays which must periodically release and retrieve each trapped particle. Additionally, the lower peak intensities required for continuously illuminated traps are less damaging to sensitive samples [14].

Similar rearrangements also would be possible with previous dynamic HOT implementations [10]. These studies used fast Fourier transforms to optimize the projected intensity over the entire trapping plane, and routinely achieved theoretical efficiencies exceeding 95% [7]. However, the discrete transforms adopted here allow us to encode more general patterns of traps.

Dynamic holographic optical tweezers need not be limited to planar configurations. If the laser beam illuminating the SLM were slightly diverging, then the entire pattern of traps would come to a focus downstream of the focal plane. Such divergence can be introduced with a Fresnel lens, encoded as a phase grating with

$$\varphi_z(\vec{\rho}) = \frac{2\pi\rho^2 z}{\lambda f^2} \quad \mod 2\pi, \tag{5}$$

where $z$ is the desired displacement of the optical traps relative to the focal plane in an optical train with effective focal length $f$. Rather than placing a separate Fresnel lens into the input beam, the same functionality can be obtained by adding the lens' phase modulation to the existing kinoform: $[(\varphi(\vec{\rho}) + \varphi_z(\vec{\rho})] \mod 2\pi$. Fig. 3(a) shows a typical array of optical tweezers collectively displaced out of the plane in this manner. The accessible range of

out-of-plane motion in our system is approximately $\pm 10$ μm.

Instead of being applied to the entire trapping pattern, separate lens functions can be applied to each trap individually with kernels

$$K_j^z(\vec{r}_j, \vec{\rho}) = \exp\left(i\frac{2\pi\rho^2 z_j}{\lambda f^2}\right) \tag{6}$$

in Eqs. (1) and (3). Fig. 3(b) shows spheres being moved independently through multiple planes in this way.

Other phase modifications implement additional functionality. For example, the phase profile

$$\varphi_\ell(\vec{\rho}) = \ell\theta \quad \mod 2\pi \tag{7}$$

converts an ordinary Gaussian laser beam into a Laguerre–Gaussian mode [15], and its corresponding optical tweezer into a so-called optical vortex [16–18]. Here $\theta$ is the polar coordinate in the DOE plane (see Fig. 1) and the integer $\ell$ is the beam's topological charge [15].

Because all phases are present along the circumference of a Laguerre–Gaussian beam, destructive interference cancels the beam's intensity along its axis. Optical vortices thus appear as bright rings surrounding dark centers. Such dark traps have been demonstrated to be useful for trapping reflecting, absorbing [19] or low-dielectric particles [18] not otherwise compatible with conventional optical tweezers.

Adding $\varphi_\ell(\vec{\rho})$ to a kinoform encoding an array of optical tweezers yields an array of identical
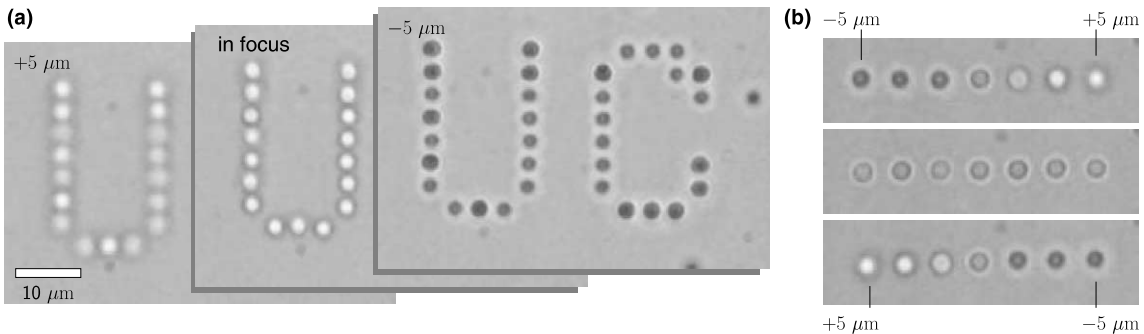


Fig. 3. Three-dimensional motion with holographic optical tweezers. The images in (a) show 34 silica spheres 0.99 μm in diameter trapped in a single plane and then displaced by $\pm 5$ μm using Eq. (5). The spheres' images change as they move relative to the focal plane. (b) Seven spheres trapped and moved independently through seven different planes using kinoforms calculated with Eq. (6).

optical vortices, as shown in Fig. 4(a). Here, the light from the array of traps is imaged by reflection off a front-surface mirror placed in the microscope's focal plane. The vortex-forming phase function also can be applied to individual traps through

$$K_j^l(\vec{r}_j, \vec{\rho}) = \exp(i\ell_j\theta) \qquad (8)$$

as demonstrated in the mixed array of optical tweezers and optical vortices shown in Fig. 4(b).

Previous reports of optical vortex trapping have considered Laguerre–Gaussian modes with relatively small topological charges, $\ell \leqslant 5$. The $\ell = 30$ examples in Fig. 4(b) are thus the most highly charged optical vortices so far reported, and traps with $\ell > 100$ are easily created with the present system.

Fig. 4(c) shows multiple colloidal particles trapped on the bright circumferences of a $3 \times 3$ array of $\ell = 15$ vortices. Because Laguerre–Gaussian modes have helical wavefronts, particles trapped on optical vortices experience tangential forces [19]. Optical vortices are useful, therefore, for driving motion at small length scales, for example in microelectromechanical systems (MEMS). Particles trapped on a vortex's bright circumference, such as the examples in Fig. 4(c) circulate rapidly around the ring, entraining cir-

culating fluid flows as they move. The resulting hydrodynamic coupling influences particles' motions on single vortices and leads to cooperative motion in particles trapped on neighboring vortices. The resulting fluid flows can be reconfigured dynamically by changing the topological charges, intensities and positions of optical vortices in an array, and may be useful for microfluidics and lab-on-a-chip applications.

The vortex-forming kernel $K^\ell$ can be combined with $K^z$ to produce three-dimensional arrays of vortices. Such heterogeneous trapping patterns are useful for organizing disparate materials into hierarchical three-dimensional structures and for exerting controlled forces and torques on extended dynamical systems.

While the present study has demonstrated how a single Gaussian laser beam can be modified to create three-dimensional arrays of optical tweezers and optical vortices, other generalizations follow naturally, with virtually any mode of light having potential applications. For example, the axicon phase profile $\varphi_\gamma(\vec{\rho}) = \gamma\rho$ creates an approximation of a Bessel mode which focuses to an axial line trap whose length is controlled by $\gamma$ [20]. These and other generalized trapping modes will be discussed elsewhere. Linear combinations of optical vortices and conventional tweezers have been shown to
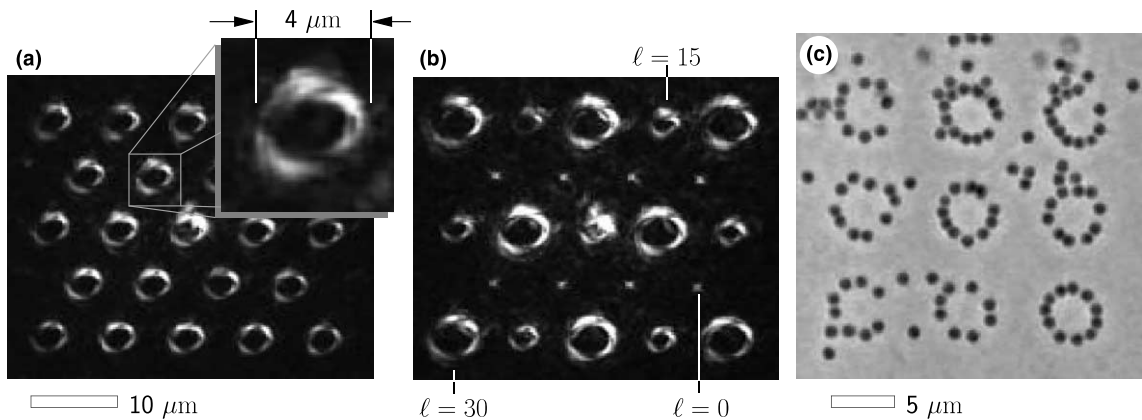


Fig. 4. (a) Triangular array of optical vortices with topological charge $\ell = 20$ created from an equivalent array of tweezers using Eq. (7). Light from the focused optical vortices is imaged by reflection from a mirror in the sample plane. The inset shows a more detailed view of one vortex's structure. (b) Mixed array of optical tweezers ($\ell = 0$) and optical vortices with $\ell = 15$ and $\ell = 30$ in the same configuration as (a), calculated with Eq. (8). The traps' amplitudes $\alpha_j$ were adjusted for uniform brightness. (c) Colloidal polystyrene spheres 800 nm in diameter trapped in $3 \times 3$ square array of $\ell = 15$ optical vortices.

operate as optical bottles [21] and controlled rotators [22]. All such trapping modalities can be combined dynamically using the techniques described above.

The complexity of realizable trapping patterns is limited in practice by the need to maintain three-dimensional intensity gradients for each trap, and by the maximum information content that can be encoded accurately in the SLM. For example, the former consideration precludes forming a three-dimensional cubic optical tweezer array with a lattice constant much smaller than 10 μm, while the latter limits our optical vortices to $\ell \approx 200$.

Within such practical bounds, dynamic holographic optical tweezers are highly reconfigurable, operate non-invasively in both open and sealed environments, and can be coupled with computer vision technology to create fully automated systems. A single apparatus thus can be adapted to a wide range of applications without modification. Dynamic holographic optical tweezers have a plethora of potential biotechnological applications including massively parallel high throughput screening, sub-cellular engineering, and macromolecular sorting. In materials science, the ability to organize materials into hierarchical three-dimensional structures constitutes an entirely new category of fabrication techniques. As research tools, dynamic holographic optical tweezers combine the demonstrated utility of optical tweezers with unprecedented flexibility and adaptability.

## Acknowledgements

## References

[1] A. Ashkin, J.M. Dziedzic, J.E. Bjorkholm, S. Chu, Opt. Lett. 11 (1986) 288.
[2] K. Svoboda, S.M. Block, Annu. Rev. Biophys. Biomol. Struct. 23 (1994) 247.
[3] A. Ashkin, IEEE J. Sel. Top. Quantum Electron. 6 (2000) 841.
[4] D.G. Grier, Curr. Opin. Colloid Interface Sci. 2 (1997) 264.
[5] E.R. Dufresne, D.G. Grier, Rev. Sci. Instrum. 69 (1998) 1974.
[6] D.G. Grier, E.R. Dufresne, US Patent 6,055,106, The University of Chicago (2000).
[7] E.R. Dufresne et al., Rev. Sci. Instrum. 72 (2001) 1810.
[8] D.G. Grier, Nature 393 (1998) 621.
[9] M. Reicherter, T. Haist, E.U. Wagemann, H.J. Tiziani, Opt. Lett. 24 (1999) 608.
[10] J. Liesener, M. Reicherter, T. Haist, H.J. Tiziani, Opt. Commun. 185 (2000) 77.
[11] Y. Igasaki et al., Opt. Rev. 6 (1999) 339.
[12] R.W. Gerchberg, W.O. Saxton, Optik 35 (1972) 237.
[13] K. Sasaki et al., Opt. Lett. 16 (1991) 1463.
[14] K.C. Neuman et al., Biophys. J. 77 (1999) 2856.
[15] N.R. Heckenberg et al., Opt. Quantum Electron. 24 (1992) S951.
[16] H. He, N.R. Heckenberg, H. Rubinsztein-Dunlop, J. Mod. Opt. 42 (1995) 217.
[17] N.B. Simpson, L. Allen, M.J. Padgett, J. Mod. Opt. 43 (1996) 2485.
[18] K.T. Gahagan, G.A. Swartzlander Jr., Opt. Lett. 21 (1996) 827.
[19] H. He, M.E.J. Friese, N.R. Heckenberg, H. Rubinsztein-Dunlop, Phys. Rev. Lett. 75 (1995) 826.
[20] J. Arlt, V. Garces-Chavez, W. Sibbett, K. Dholakia, Opt. Commun. 197 (2001) 239.
[21] J. Arlt, M.J. Padgett, Opt. Lett. 25 (2000) 191.
[22] L. Paterson et al., Science 292 (2001) 912.